Journal of Alloys and Compounds 499 (2010) 121–125

Contents lists available at ScienceDirect

Journal of Alloys and Compounds

journal homepage: www.elsevier.com/locate/jallcom

Solution-chemical syntheses of nanostructure HgTe via a simple hydrothermal process

Masoud Salavati-Niasari[a,b,*], Mehdi Bazarganipour[b], Fatemeh Davar[a]

[a] Institute of Nano Science and Nano Technology, University of Kashan, Kashan, P.O. Box 87317–51167, I. R. Iran
[b] Department of Inorganic Chemistry, Faculty of Chemistry, University of Kashan, Kashan, P.O. Box 87317–51167, I. R. Iran

ARTICLE INFO

Article history:
Received 19 December 2009
Received in revised form 12 March 2010
Accepted 15 March 2010
Available online 23 March 2010

Keywords:
Hydrothermal
HgTe
Nanostructure
Solution-chemical

ABSTRACT

HgTe rod-shape composed of crystalline particles has been prepared by a hydrothermal method, and characterized by means of X-ray powder diffraction (XRD), scanning electron microscopy (SEM), and transition electron microscopy (TEM). The effects of capping agents, reductants, reaction temperatures, and reaction times on crystal structures and shapes of HgTe have been investigated. The results showed that the CTAB as capping agent plays a crucial role in the hydrothermal process. The synthesis procedure is simple and uses less toxic reagents than the previously reported methods.

1. Introduction

Recently, nanocrystalline chalcogenides of the late transition metals and the main group elements have attracted much interest due to their unique thermoelectric, semiconducting and optical properties. Most studies in this area were focused on cadmium and zinc compounds [1–3]. On the other hand, only a few publications have reported the synthesis of mercury sulfides, selenides and tellurides, mostly due to the high toxicity of mercury. Nevertheless, mercury chalcogenides are promising materials for catalysts, infrared detectors [4], light emitting diodes and electrochemical cells [5,6]. In particular, nanocrystalline HgTe is one of the candidate materials in the area of photoconductive/photovoltaic devices, IR detectors and IR emitters [7].

While II–VI semiconductor NCs such as CdSe have been prepared routinely and extensively studied, the synthesis of mercury chalcogenide QDs have still remained a challenge. Of these chalcogenides, HgTe is of interest for applications in the optoelectronics industry, since its emission covers the low-loss transmission windows in silica telecommunication fibers, which lies at around 1300 nm (0.95 eV) and 1550 nm (0.79 eV) [8]. As a bulk material, HgTe exists as a semi-metal with a negative band gap of 20.15 eV [9]. If this material is made in the form of small particles and quantum confinement occurs, the band gap will widen and the material may exhibit properties of a narrow band gap semiconductor with potential optical properties at the telecommunications wavelengths. Also it is worthy to note that excitonic diameter in HgTe is large.

Due to the population with highly mobile carriers, HgTe is an ideal material in semiconductor devices such as optical switches, infrared detectors or photovoltaics [10–12]. Several methods have been applied for preparation of conventional HgTe materials including the combination of the elements at elevated temperature [13], molecular precursor method [14], and organometallic vapor phase epitaxy growth [15,16]. Recently, vigorous interest has been intrigued by nanometer-scaled HgTe particle because of its quantum confinement effect which can dramatically increase the effective band gap and give rise to near-infrared emission, suggesting prospective applications in 1.3 and 1.5 μm optical telecommunication devices [17–23].

Li et al. have prepared mercury chalcogenides HgE (E = S, Se, Te) with spherical morphologies by conversion of HgO with chalcogen in ethylenediamine at room temperature [17]. Song et al. have reported a sonochemical method of synthesizing nanocrystalline HgTe in which ethylenediamine was used as solvent but mixed with a complexing agent of 1-thioglycerol [18]. Wet chemical synthetic routes have also been developed for colloidal HgTe nanoparticles in aqueous solution at room temperature [19–21].

* Corresponding author at: Institute of Nano Science and Nano Technology, University of Kashan, Kashan, P.O. Box 87317–51167, Islamic Republic of Iran. Tel.: +98 361 5555 333; fax: +98 361 5552 930.
E-mail address: salavati@kashanu.ac.ir (M. Salavati-Niasari).

0925-8388/$ – see front matter © 2010 Elsevier B.V. All rights reserved.
doi:10.1016/j.jallcom.2010.03.135

2. Experimental

2.1. Materials and physical measurements

All of reagents and solvents were purchased from Merck (pro-analysis) and were dried using molecular sieves (Linde 4 Å). XRD patterns were recorded by a Rigaku D-max C III, X-ray diffractometer using Ni-filtered Cu Kα radiation. Scanning electron microscopy (SEM) images were obtained on Philips XL-30ESEM equipped with an energy dispersive X-ray (EDX). Transmission electron microscopy (TEM) images were obtained on a Philips EM208 transmission electron microscope with an accelerating voltage of 100 kV.

2.2. Nanostructure HgTe prepared by hydrothermal method

$Hg(NO_3)_3{\cdot}H_2O$ and $TeCl_4$ were used as the simple precursor in the hydrothermal synthesis. The precursor with stoichiometric ratio of Hg:Te (1:1) was put into a Teflon-lined autoclave. The autoclave was then filled with water up to 80% of its volume. After adding sufficient KBH_4 as the reductant, NaOH as base and PEG 20,000 as capping agent, the autoclave was sealed immediately and heated to 180 °C for the synthesis reaction. After reaction for 12 h, the autoclave was cooled down to room temperature naturally. The obtained precipitates were separated by centrifugation, washed with deionized water followed by ethanol for three times, and dried at 100 °C under vacuum for 24 h. The structure and morphology of the HgTe powders were characterized by XRD and TEM.

3. Results and discussion

The reaction of mercury(II) nitrate with $TeCl_4$ in presence of PEG 20,000 and KBH_4 as described above resulted in the formation of nanosized cubic HgTe [space group: *F-43m* (2 1 6)]. The particles were crystalline, as determined by powder X-ray diffraction (XRD) measurements shown in Fig. 1a. The wide-angle peaks indicate the cubic phase and correspond to diffractions from the 1 1 1, 2 2 0, and 3 1 1 planes of bulk HgTe coloradoite. The peaks are broadened compared to those of bulk HgTe, indicating the small particle size. The crystallite size diameter (D) of the HgTe nanoparticles has been calculated by Debye–Scherrer equation:

$$D = \frac{0.9\lambda}{\beta \cos\theta}$$

where β-FWHM (full-width at half-maximum, or half-width) is in radians and θ is the position of the maximum of diffraction peak and λ is the X-ray wavelength (1.5406 Å for Cu Kα). The mean size of the particles was estimated 34 nm (JCPDS 77-2014). No remarkable diffractions of other phases such as tellurium, mercury or their other compounds can be found in Fig. 1a, indicating that a pure HgTe phase has been formed after the synthesis for the samples.

Meanwhile, influence of capping agent, reductant sort, temperature and time were investigated on the as-prepared nanostructure HgTe (Fig. 1b–e). With exchange of capping agent from PEG 20,000 to CTAB (cetyltrimethylammoniumbromide) and reductant sort from KBH_4 to N_2H_4, particle size of 34–27 nm was decreased, respectively (Fig. 1a and b). In other word, with increasing of time from 12 to 24 h, particle size was increased from 27 to 35 nm, respectively (Fig. 1b and c). At the same time, with decreasing of temperature from 180 to 120 °C, further peaks were observed that exhibited impurity in nanostructure HgTe (showed with triangles in pattern) (Fig. 1d). Obviously, the crystallinity of the as-prepared HgTe gradually improved with increasing reaction temperature and time. In general, the resultant particles became bigger with increasing temperature and time.

The morphology and size of the as-synthesized products were characterized by SEM and TEM. Fig. 2a and b depicts SEM and TEM images of sample nanostructure HgTe in presence of KBH_4 as reductant and PEG 20,000 as capping agent at 180 °C and 12 h. From the micrograph, it was observed that the nanostructure was slightly agglomerated. Fig. 2c and d reveals reductant sort effect on morphology of nanostructures in presence of PEG 20,000 as capping agent. In this study, reductant plays the key role on morphology of nanostructure HgTe. In presence of N_2H_4 as reductant, the rod-shape shape is preferential morphology along with agglomeration of particles (Fig. 2c). Meanwhile, in presence of Zn as reductant, particles are highly agglomerated (Fig. 2d).

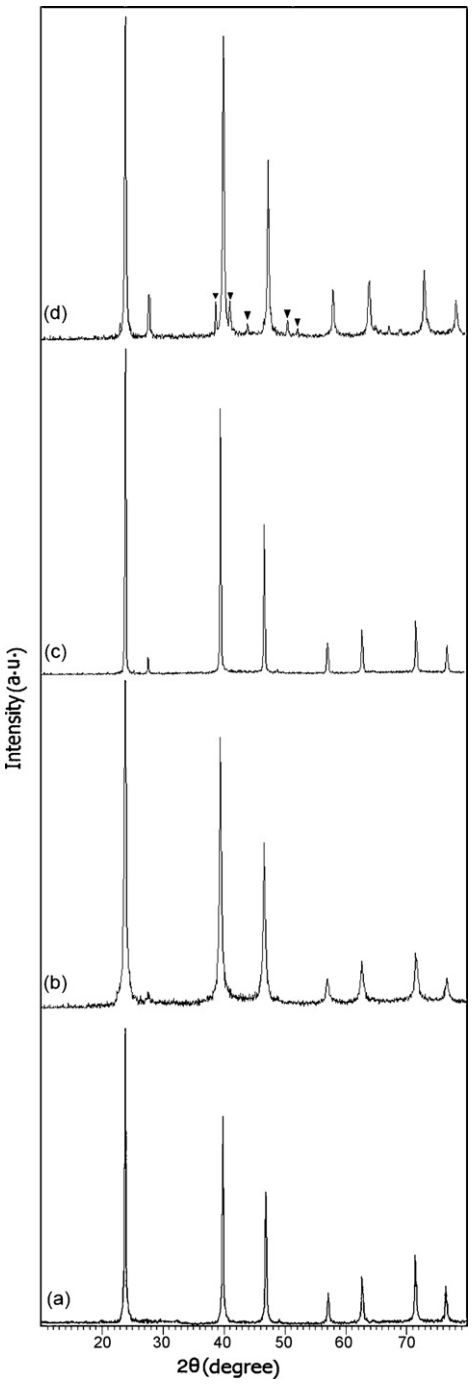

Fig. 1. XRD patterns of prepared HgTe in (a) 180 °C and 12 h, at the presence of PEG 20,000 as capping agent and KBH_4 as reductant, (b) CTAB as capping agent and N_2H_4 as reductant, (c) CTAB as capping agent, N_2H_4 as reductant and 24 h and (d) CTAB as capping agent, N_2H_4 as reductant, 24 h and 120 °C.

The strong reductant KBH_4 and N_2H_4 in combination with stirring rapidly created a large number of nuclei and further growth of the nuclei was limited. As a result, many small particles were obtained. The reduction at the presence of Zn proceeds only two-dimensionally, i.e., at the interface of Zn powder with the metal cation solution. The rate of reduction is further limited by the mass transport of the metal cation solution to the Zn surface. Therefore, depletion of metal cations near the interface might occur. As a con-

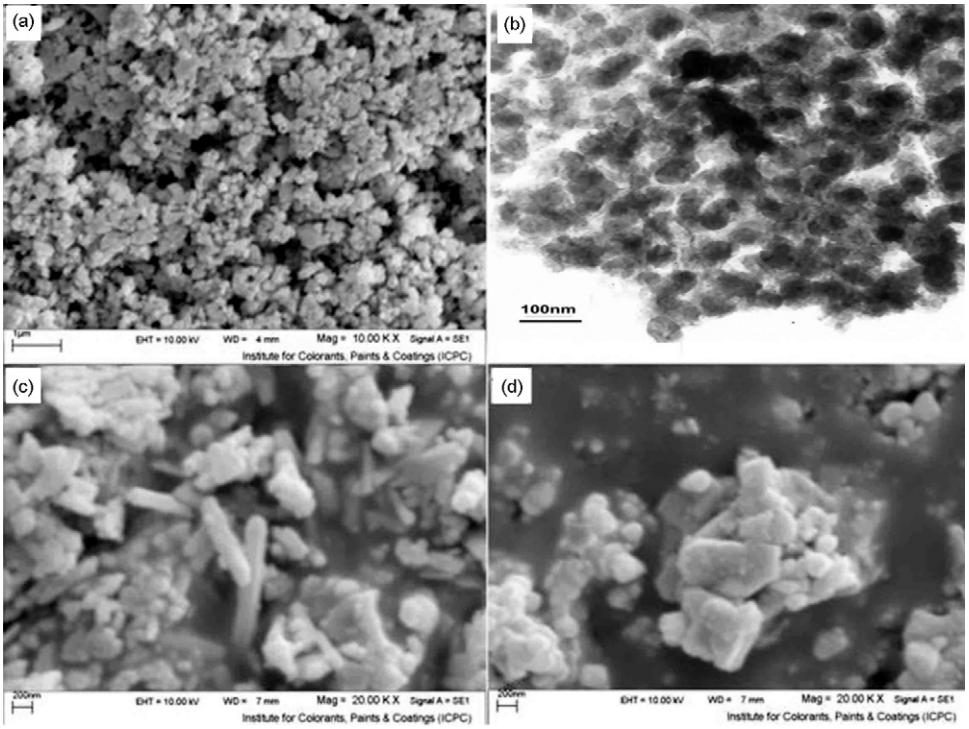

Fig. 2. (a and b) SEM and TEM image of images of HgTe in presence of KBH_4 as reductant and PEG 20,000 as capping agent at 180 °C and (c and d) SEM images of HgTe in presence of CTAB as capping agent and N_2H_4 and Zn as reductant, respectively.

sequence of the rate and surface area limitation, crystal growth is favored over nucleus formation as the result of larger particles [24].

On the other hand, to reach ideal morphology, we prepared nanostructure HgTe with various capping agents such as: CTAB and SDBS (sodium dodecyl-benzene-sulfonate) in the presence of N_2H_4 as reductant (Fig. 3a and b). Fig. 3a and b shows that, utilization of CTAB, rod-shape is preferential morphology; meanwhile, utilization of SDBS as capping agent inclines agglomeration of nanostructure and growing of particle. Experiments showed that the morphology of the final product could be affected by Hg^{2+} ion sources (Fig. 3c and d). Keeping the other experimental conditions constant, however, SEM observations showed that the morpholo-

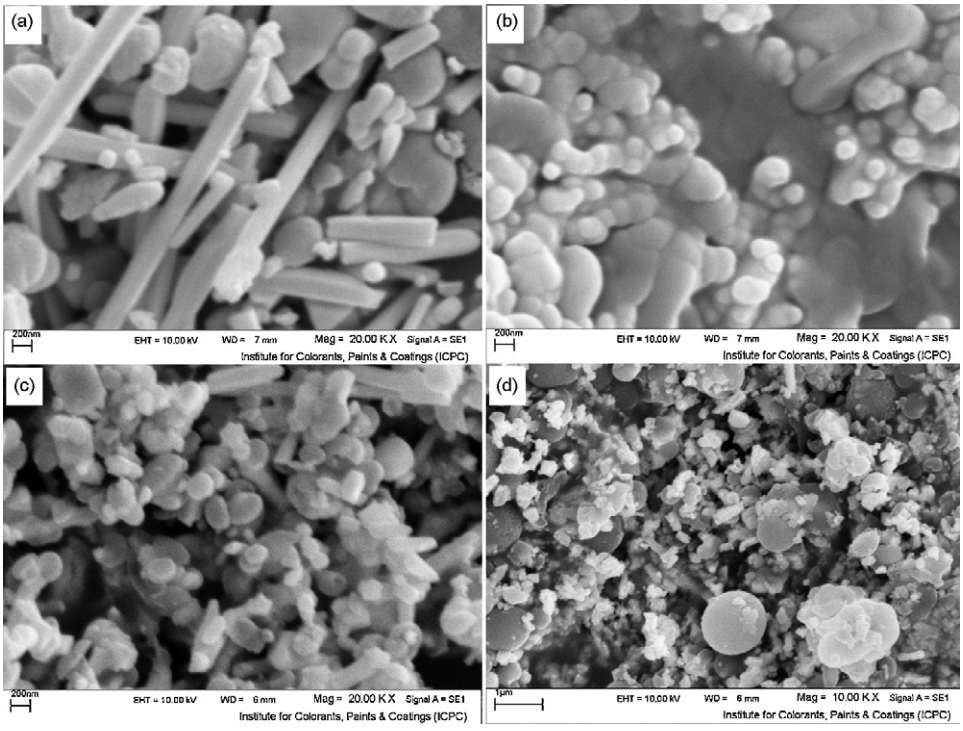

Fig. 3. SEM images of HgTe in presence of (a) CTAB and (b) SDBS as capping agent, in 180 °C, 12 h and N_2H_4 as reductant and (c) $HgCl_2$ and (d) $HgSO_4$ as source of Hg^{2+} in presence of CTAB as capping agent 180 °C, 12 h and N_2H_4 as reductant.

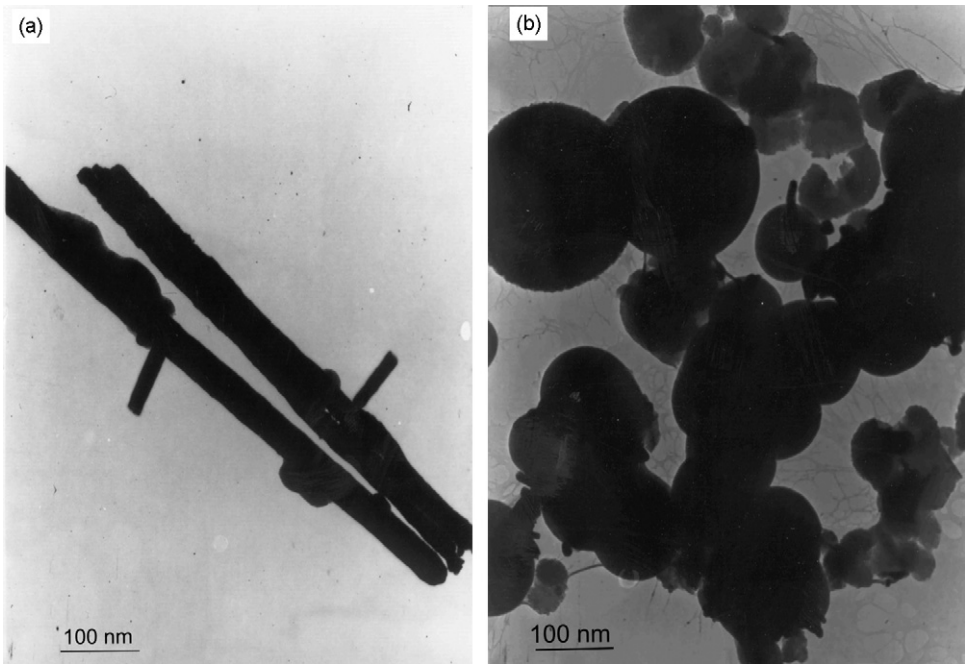

Fig. 4. TEM images of HgTe of (a) CTAB as capping agent, in 180 °C, 12 h and N_2H_4 as reductant and (b) $HgSO_4$ as source of Hg^{2+} in presence of CTAB as capping agent 180 °C, 12 h and N_2H_4 as reductant.

gies of the products were obviously different. When $HgCl_2$ was used as Hg^{2+} ion source, some rod-shape nanostructures were replaced by particles (Fig. 3c). When $HgSO_4$ was used, many HgTe irregular particles were produced (Fig. 3d).

In Fig. 4, we illustrated TEM images of HgTe in presence of CTAB as capping agent, N_2H_4 as reductant (Fig. 4a) and $HgSO_4$ as source of Hg^{2+} (Fig. 4b).

With variation base from NaOH to NH_3 with keeping the other experimental conditions constant, we observed morphology of nanostructure exchanged from rod-shape to shuck-like (Fig. 5a). Meanwhile, with increasing reaction time from 12 to 24 h, nanostructures showed dense agglomerate and particle size was increased (Fig. 5b). Fig. 5c shows temperature effect on HgTe morphology. With decreasing temperature from 180 to 120 °C some rod-shape nanostructures together with impurity were obtained (Figs. 5b and 1d). Also, nanostructure HgTe was prepared at room temperature in presence of CTAB as capping agent and N_2H_4 as reductant (Fig. 5d). At room temperature, rod-shape nanos-

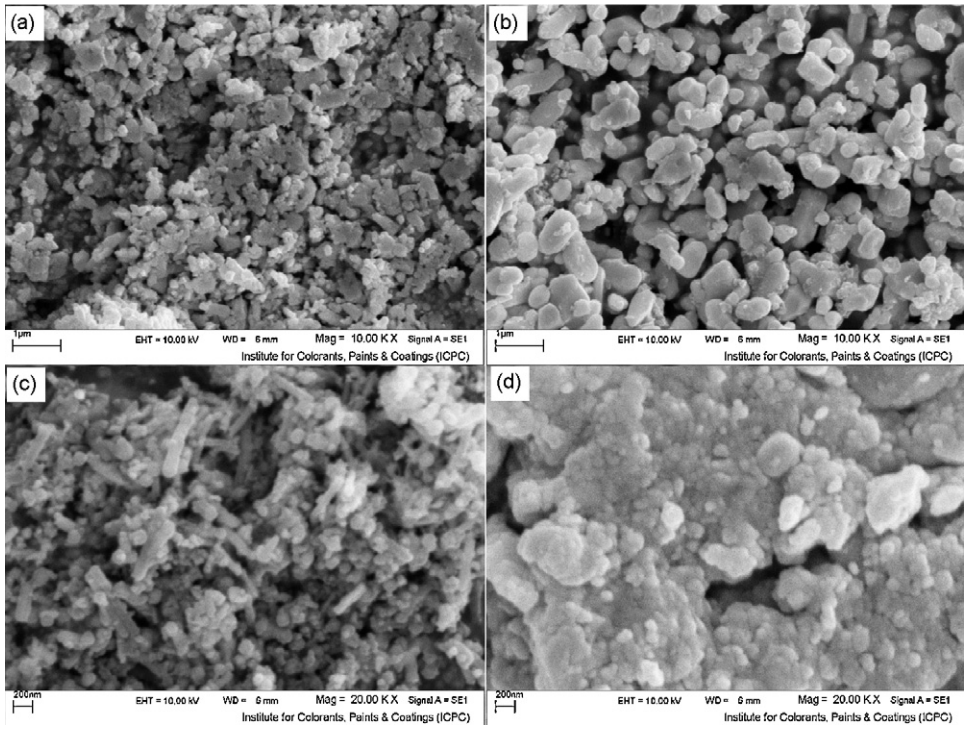

Fig. 5. SEM images of HgTe: (a) NH_3 as base, 12 h and 180 °C; (b) 24 h, 180 °C; (c) 120 °C, 12 h; and (d) room temperature, 12 h in presence of CTAB as capping agent and N_2H_4 as reductant.

Table 1
Characterization comparison of HgTe nanostructures with other similar works.

Method	Precursors	Size	Morphology	Ref.
Hydrothermal	$HgCl_2$, Na_2TeO_3	Diameter of 100–300 nm and length of up to 2–3 μm	Nanorods	[25]
Sonochemical	$Hg(ClO_4)_2$, tellurium powder	Diameters of 15 nm and lengths of up to 200 nm	Nanorods	[18]
Sonochemical	$Hg(NO_3)_2$, tellurium powder	65 nm	Nanoparticles	[26]
Solution method	HgO, Te powder	2.3 nm	Nanocrystals	[27]

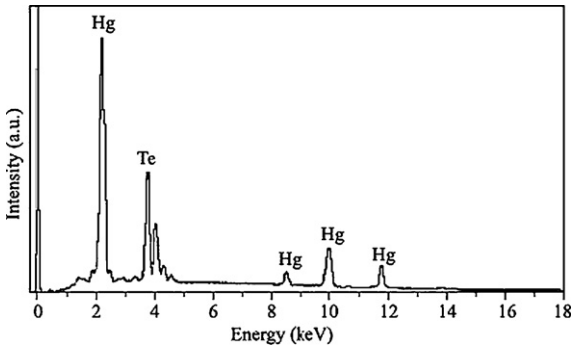

Fig. 6. EDX spectrum of the HgTe nanoparticles prepared in the presence of KBH_4 as reductant and PEG 20,000 as capping agent at 180 °C.

tructures are broken down and agglomerated similar to HgTe bulk.

The EDX analysis of the product, prepared HgTe in the presence of KBH_4 as reductant and PEG 20,000 as capping agent at 180 °C, is shown in Fig. 6, in which only Hg and Te-related peaks are present with the atomic ratio close to 1 [18]. The EDX spectra for other samples were similar as with the spectra shown in Fig. 6.

In comparison to other similar works that illustrated in Table 1, our method is simple and has low cost and scale-up route. Also, we have used nontoxic precursors and solvent. In this route, we apply various capping agents and sort of reductants which are rare in preparation of nanostructure HgTe and rod-shape morphology was obtained. The sizes of nanostructure HgTe seem convenient than similar works.

4. Conclusion

In summary, this work has demonstrated a new approach for the controllable growth of HgTe rod-shape via exchange reductant and capping agent. This route to HgTe nanostructure is simple, convenient, effective, and holds potential for large-scale synthesis needed for commercial applications. Most important of all, the new approach can yield rod-shape morphology of HgTe directly without the mechanical crushing and the sieving needed for a solidified melt which may exhibit enhanced near-infrared properties.

Acknowledgment

Authors are grateful to Council of Institute of Nano Science and Nano Technology, University of Kashan and for providing financial support to undertake this work.

References

[1] C.B. Murray, D.J. Norris, M.G. Bawendi, J. Am. Chem. Soc. 115 (1993) 8706–8715.
[2] K. Sooklal, B.S. Cullum, S.M. Angel, C.J. Murphy, J. Phys. Chem. 100 (1996) 4551–4555.
[3] M. Fromment, H. Cachet, H. Essaaidi, G. Maurin, R. Cortes, Pure Appl. Chem. 69 (1997) 77–82.
[4] G. Debias, Phys. Status Solid A 83 (1984) 269–278.
[5] V.L. Colvin, M.C. Schlamp, A.P. Aliviastors, Nature 370 (1994) 354–357.
[6] A. Hangfeldt, M. Gratzel, Chem. Rev. 95 (1995) 49–68.
[7] S.S. Kale, C.D. Lockhande, Mater. Chem. Phys. 59 (1999) 242–246.
[8] M.T. Harrison, S.V. Kershaw, M.G. Burt, A.L. Rogach, A. Kornowski, A. Eychmüller, H. Weller, Pure Appl. Chem. 72 (2000) 295–307.
[9] Landolt-Börnstein, Numerical Data and Functional Relationships in Science and Technology: New Series, vol. 17b: Semiconductors, Springer, Berlin, 1982.
[10] A. Delin, T. Klüner, Phys. Rev. B 66 (2002) 035117–035124.
[11] N.G. Wright, M.I. McMahon, R.J. Nelmes, Phys. Rev. B 48 (1993) 13111–13114.
[12] V. Daumer, L. Golombek, M. Gbordzoe, E.G. Novik, V. Hock, C.R. Becker, H. Buhmann, L.W. Molenkamp, Appl. Phys. Lett. 83 (2003) 1376–1378.
[13] T. Nath, S. Roy, P. Saxena, P.C. Mathur, J. Appl. Phys. 67 (1990) 826–831.
[14] M.L. Steigerwald, C.R. Sprinkle, J. Am. Chem. Soc. 109 (1987) 7200–7201.
[15] R. Korenstein, W.E. Hoke, P.J. Lemonias, J. Appl. Phys. 62 (1987) 4929–4931.
[16] S.K. Ghandhi, I.B. Bhat, H. Ehsani, D. Nucciarone, G. Miller, Appl. Phys. Lett. 55 (1989) 137–139.
[17] Y.D. Li, Y. Ding, H.W. Liao, Y.T. Qian, J. Phys. Chem. Solids 60 (1999) 965–968.
[18] H. Song, K. Cho, H. Kim, J.S. Lee, B. Min, H.S. Kim, S.W. Kim, T. Noh, S. Kim, J. Cryst. Growth 269 (2004) 317–323.
[19] M.T. Harrrison, S.V. Kershaw, A.L. Rogach, A. Kornowski, A. Eychmüller, H. Weller, Adv. Mater. 12 (2000) 123–125.
[20] M. Green, G. Wakefield, P.J. Dobson, J. Mater. Chem. 13 (2003) 1076–1078.
[21] H. Kim, K. Cho, H. Song, B. Min, J.-S. Lee, G.-T. Kim, S. Kim, Appl. Phys. Lett. 83 (2003) 4619–4621.
[22] P. Olk, B.C. Buchler, V. Sandoghdar, N. Gaponik, A. Eychmüller, A.L. Rogach1, Appl. Phys. Lett. 84 (2004) 4732–4734.
[23] M. Kazes, D.Y. Lewis, Y. Ebenstein, T. Mokari, U. Banin, Adv. Mater. 14 (2002) 317–321.
[24] A. Trifonova, M. Wachtler, M.R. Wagner, H. Schroettner, C. Mitterbauer, F. Hofer, K.-C. Möller, M. Winter, J.O. Besenhard, Solid State Ionics 168 (2004) 51–59.
[25] A.-M. Qin, Y.-P. Fang, C.-Y. Su, Mater. Lett. 61 (2007) 126–129.
[26] M. Kristl, M. Drofenik, Ultrasonics Sonochem 15 (2008) 695–699.
[27] L.S. Li, H. Wang, Y. Liu, S. Lou, Y. Wang, Z. Du, J. Colloid Interface Sci. 308 (2007) 254–257.